LES of a high Reynolds, high subsonic jet : effects of the inflow conditions on flow and noise.*

Christophe Bogey[†] and Christophe Bailly[‡]

Laboratoire de Mécanique des Fluides et d'Acoustique
Ecole Centrale de Lyon & UMR CNRS 5509
69134 Ecully, France.

Abstract

Large Eddy Simulations of a circular jet with a Mach number M = 0.9 and a Reynolds number $\mathrm{Re}_D = 4 \times 10^5$ are performed to investigate the effects of the inflow conditions on flow development and sound field. Initial parameters of an earlier simulation[1] using a ring vortex excitation involving several azimuthal modes[2] are changed: the forcing amplitude, the shear layer thickness and the use of the first modes in the excitation. The most significant modifications in the jet features are found in the latter case: when the first four azimuthal modes are removed from the forcing, the jet develops much slower with reduced turbulence intensities and the jet is quieter. Moreover, links between the sound levels and the turbulence intensity peaks are observed: downstream sound levels vary as the peak amplitudes of centerline turbulence intensities, and sideline levels as those of the fluctuating radial velocity in the shear layer.

1. Introduction

At the end of the seventies, experiments were conducted to reduce jet noise thanks to shear-layer artificial excitation. Given contradictory results, Crighton[3] observed that the broadband noise was suppressed below a Reynolds number Re_D of about 10^5, but amplified for higher Re_D. The presence of such a barrier Reynolds number was clarified by noting that its value corresponds to this below which the jet exit shear layer is fully laminar,[4] which demonstrated that jet noise mechanisms depend on the shear-layer initial state. These works on excited jets illustrate that jet noise may change according to the initial conditions. This issue is still to be investigated to better understand the physics of sound generation. It must be also taken into account for the modelling of inflow conditions in jet noise simulations.

Experimentally, the influence of initial conditions on jet flow has usually been studied for jets with Reynolds numbers about $10^5 < Re_D < 5 \times 10^5$. In this range, the exit shear layer is expected to be transitional, but the use of tripping devices in the nozzle can make it go fully turbulent. Hill & Jenkins[5] thus described that flow characteristics of plane jets were sensitive to changes in the apparatus in the initially laminar but not in the turbulent case. A similar sensitivity was found for round jets by Gutmark & Ho[6] who reported that initial conditions of laminar shear layers were changed by extremely low-level spatially coherent disturbances in facilities. Measures of axisymmetric free shear layers were documented by Hussain *et al.*[7–9] for different initial conditions. The parameters in the self-preserving region were shown to be essentially dependent on whether the initial shear layer is transitional or turbulent, whereas the distance required for reaching this region depends noticeably on the initial shear layer thickness. As for the effects of the initial shear layer state on the flow itself, they were investigated for round jets by Raman *et al.*[10] or Xu & Antonia.[11] The jet development was found to be much more rapid in the initially transitional than in the turbulent case.

The influence of exit conditions on subsonic jet noise has also been studied. Bridges & Hussain[12] reported that a circuler jet at $\mathrm{Re}_D = 1.5 \times 10^5$ was 2.5 dB quieter when tripping its initial shear layer. Devices acting on the noise producing region have been tested with the aim of sound reduction. Simonich *et al.*[13] used tabs for a circular jet at $\mathrm{Re}_D = 1.7 \times 10^6$ to enhance near-field jet mixing, while Arakeri *et al.*[14] used micro-jets at

[†]Research scientist CNRS, email: christophe.bogey@ec-lyon.fr

[‡]Assistant Professor, Member AIAA, email: christophe.bailly@ec-lyon.fr

$\mathrm{Re}_D = 5 \times 10^5$ and observed significant lowering in the near-field turbulent intensities. In the two cases, the sound levels decreased by about 2 dB.

In simulations, real exit conditions[4] can not be reproduced since the discretization of the shear layers leads to a prohibitive number of grid points. Initial conditions must therefore be modelled. For jets, the classical approach consists in introducing random perturbations near the inflow to seed the turbulence. These can be issued from a synthetic turbulent field,[15] or be based on the jet azimuthal modes.[2] Their amplitudes are usually set to low values, particularly in noise simulations for minimizing spurious waves. Great care must be taken so that the artificial inflow conditions do not bias the results, as pointed out by Bodony & Lele[16] about a forcing using only the first three azimuthal modes of a circular jet. Moreover if Chyczewski *et al.*[17] observed that for the forcing amplitude did not significantly alter the development of a rectangular supersonic jet, Stanley & Sarkar[15] presented clearly the influence of the inflow turbulence intensity and of the shear-layer thickness for a plane subsonic jet. The dependence of the similarity parameters on the initial velocity profile was also shown by Boersma *et al.*[18] for a circular jet.

In the present paper, the effects of artificial inflow condtions on the development and the radiated sound field of a Mach number M = 0.9, circular jet are investigated. The Reynolds number $\mathrm{Re}_D = 4 \times 10^5$ is chosen to be above the barrier Reynolds number of 10^5, in the range of transitional jets where the exit shear layers still can be not fully turbulent. Such a jet was recently simulated[1] using a vortex ring inflow forcing[2] involving the first sixteen azimuthal modes. The flow and the sound field obtained directly by Large Eddy Simulation were described in detail and compared to relevant measurements. Both correspond to what is expected at a high Reynolds number supporting that the LES is Reynolds Number Preserving (RNP-LES), see for instance the study[19] reporting the effects of the subgrid modellings. In the present work, LES with inflow parameters modified with respect to the earlier simulation[1] are performed. The investigated parameters are the forcing amplitude, the initial shear layer thickness and the use of the first four azimuthal modes when synthesizing the forcing disturbances. Effects on jet flow and noise are shown, and an attempt to discuss noise sources is conducted from the LES data.

In section 2, the main features of the numerical procedure and the specifications of the different inflow conditions are given. Snapshots of vorticity and pressure are also presented. The flow fields are shown in section 3, with two subsections devoted to the shear layer zone and to the jet development. The acoustic fields are reported in section 4, and possible links with the flow properties are suggested. Finally concluding remarks are drawn in section 5.

2. Simulation parameters

2.1 Numerical procedure

The numerical algorithm is this of the earlier simulation[1] of the M = 0.9, $\mathrm{Re}_D = 4 \times 10^5$ jet. The filtered compressible Navier-Stokes equations are solved using highly accurate numerical schemes with low dispersion and low dissipation properties.[20] A thirteen-point finite-difference scheme is used for spatial discretization while an explicit six-stage Runge-Kutta algorithm is applied for time integration. Grid-to-grid oscillations are removed thanks to an explicit filtering which is optimized to only damp the short waves discretized by less than four points per wavelength. Its use allows to ensure numerical stability, but also to take into account the effects of the subgrid energy-dissipating scales without affecting the resolved scales. This approach was developed to preserve the effective Reynolds number of the jet, which might not be possible using eddy-viscosity subgrid models such as the dynamical Smagorinsky model.[19] Moreover to directly compute the noise, non-reflective boundary conditions are implemented, with the addition of a sponge zone[21] at the outflow.

The numerical parameters of the present simulations are those of the simulation referred to as LESac in a recent paper.[1] The computational domain is discretized by a 12.5 million point Cartesian grid with 15 points in the jet radius r_0. The flow is computed up to an axial distance of $25r_0$. The sound field is calculated radially up to $15r_0$ from the jet axis, and resolved for Strouhal numbers $St = fD/u_j < 2$. Finally, the simulation time T is long enough to achieve convergence of results, as shown for instance by the corresponding Strouhal number $D/(Tu_j) = 9.9 \times 10^{-4}$.

2.2 Definition of the inflow conditions

Initial conditions are defined for an isothermal round jet with a centerline velocity u_j and a diameter $D = 2r_0$ yielding a Mach number $\mathrm{M} = u_j/c_a = 0.9$ and a Reynolds number $\mathrm{Re}_D = u_jD/\nu = 4\times10^5$. The mean profiles of velocities, pressure and density are imposed at the inflow boundary. The axial velocity is given by a hyperbolic-tangent profile describing an annular shear layer of radius r_0 and of momentum thickness δ_θ. Radial and azimuthal velocities are set to zero, pressure is taken as the ambient pressure, and the mean density profile is obtained from a Crocco-Buseman relation.

To start the turbulence transition, disturbances are added to the velocity profiles in the shear layer zone. They are divergence-free and have a low amplitude to minimize spurious acoustic waves. The inflow forcing is based on a combination of the jet azimuthal modes, and it modifies the flow velocities every time step in the following way

$$\left\{ \begin{array}{c} u_x \\ u_r \end{array} \right\} = \left\{ \begin{array}{c} u_x \\ u_r \end{array} \right\} + \alpha u_j \sum_{i=n}^{m} \epsilon_i \cos(i\theta + \phi_i) \left\{ \begin{array}{c} u_x^{ring} \\ u_r^{ring} \end{array} \right\}$$

where the amplitudes $-1 \leq \epsilon_i \leq 1$ and the phases $0 \leq \phi_i \leq 2\pi$ of each mode are randomly updated every iteration. The unit vortex ring velocities are expressed, for $r = \sqrt{y^2 + z^2} \neq 0$, as

$$\left\{ \begin{array}{c} u_x^{ring} \\ u_r^{ring} \end{array} \right\} = \frac{2 r_0}{r \Delta y} \exp\left(- \ln(2) \frac{\Delta(x,r)^2}{\Delta y^2} \right) \left\{ \begin{array}{c} r - r_0 \\ x_0 - x \end{array} \right\}$$

where $\Delta(x,r)^2 = (x - x_0)^2 + (r - r_0)^2$, Δy is the transverse grid spacing, and the axial location is $x_0 \simeq r_0$. Note that a large part of the forcing disturbances is damped owing to the random updating. This forcing procedure was first used for a moderate Reynolds number jet[2] with $\alpha = 0.01$, $n = 0$ and $m = 9$.

In the present study, four simulations are carried out with the inflow conditions summarized in Table 1. The parameters ($\delta_\theta = 0.05 r_0$, $\alpha = 0.007$, $n = 0$, $m = 15$) of the simulation[1] referred to as LESac are changed in three new simulations: the amplitude α is divided by two in the LESampl simulation, the shear layer is significantly thinner in the LESshear simulation with $\delta_\theta = 0.03 r_0$, and the first four modes from $i = 0$ to 3 are removed in the forcing of the LESmode simulation.

	δ_θ / r_0	α	modes
LESac	0.05	0.007	i=0,...,15
LESampl	0.05	0.0035	i=0,...,15
LESshear	0.03	0.007	i=0,...,15
LESmode	0.05	0.007	i=4,...,15

Table 1: Inflow conditions of the different simulations.

In sections 3 and 4, profiles will be plotted to compare the computed flow and sound fields. They all will follow the line type definitions of Table 2.

LESac	———
LESampl	·······
LESshear	— — —
LESmode	— · — ·

Table 2: Line types used for the four simulation profiles.

2.3 Instantaneous vorticity and pressure

Figures 1 and 2 present snapshots of the vorticity norm and of the fluctuating pressure for the four simulations. The flow developments from transitional shear layers to turbulent jets appear fairly similar, but also more or less rapid according to the inflow conditions. The jet seems to develop faster in the LESshear simulation, and slower in the LESmode simulation. These observations are supported by the mean centerline axial velocities u_c later shown in Figure 6 and by the core lengths x_c defined here by $u_c(x_c) = 0.95 u_j$, which are given in Table 3 but discussed further.

LESac	$x_c = 10.2 r_0$
LESampl	$x_c = 10.6 r_0$
LESshear	$x_c = 9.8 r_0$
LESmode	$x_c = 11.9 r_0$

Table 3: Core lengths obtained for the different simulations.

Changes in the radiated sound fields are also visible in the pressure snapshots. Whereas the sound radiations for the LESac and for the LESampl simulations seem not to differ significantly, the radiations for the LESshear and for LESmode simulations appear to be respectively enhanced and reduced, particularly in the sideline and in the upstream directions.

3. Flow properties

3.1 Shear-layer developement

The streamwise variations of the shear layer vorticity thickness δ_ω are shown in Figure 3 for the different simulations. This characteristic thickness is calculated from the the mean axial velocity $<u>$ using $\delta_\omega = u_j / \max\left(|\partial <u> / \partial y|\right)$, and it is related to the momentum thickness for a hyperbolic-tangent profile by $\delta_\omega = 4\delta_\theta$. For the three simulations LESac, LESshear and LESampl, the shear layer spreads earlier with the smaller initial thickness as observed experimentally by Hussain & Zedan,[7] and later with the decreased forcing amplitude. Similar growth rates $d\delta_\omega / dx$ are found, with a value of about 0.22

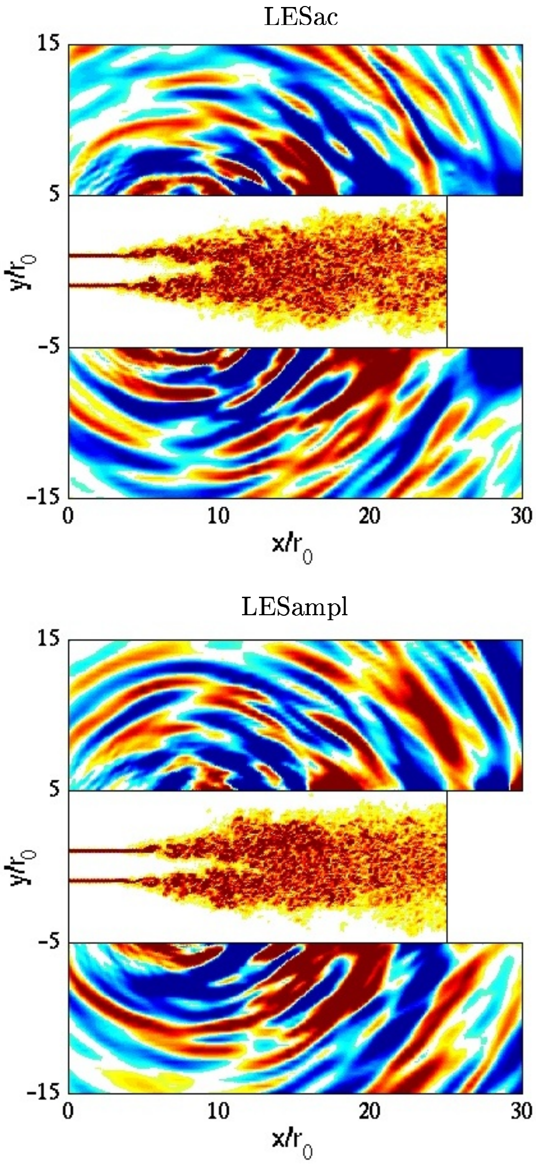

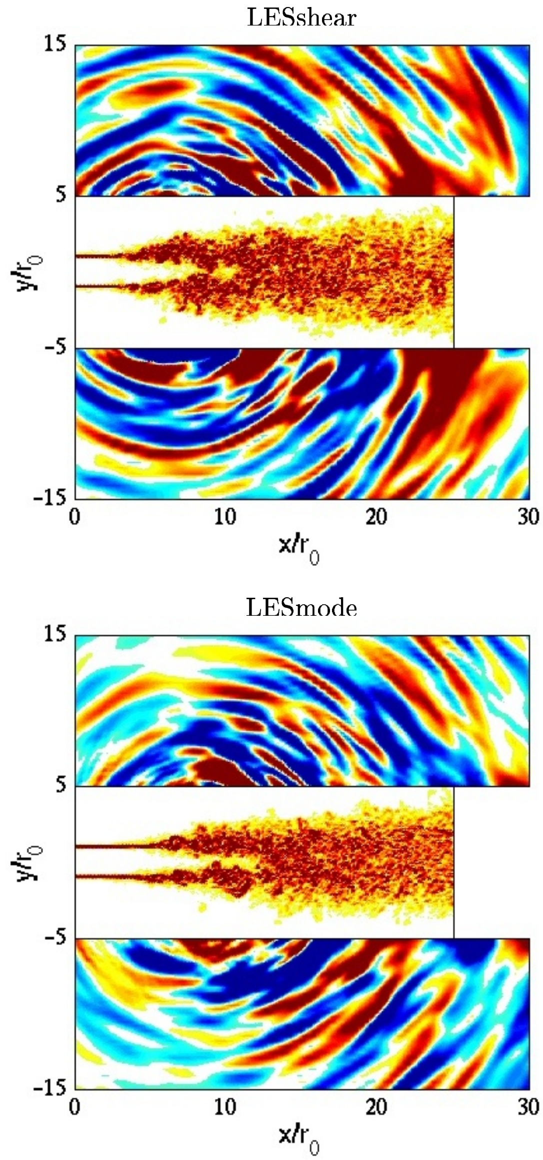

Figure 1: Snapshots of the vorticity $|\boldsymbol{\omega}|$ in the flow and of the fluctuating pressure p' outside, in the $x-y$ plane at $z=0$, for the simulations LESac and LESampl. The color scales are from 0 to 8×10^4 s^{-1} for the vorticity and from -70 to 70 Pa for the pressure.

Figure 2: Snapshots of the vorticity and of the fluctuating pressure, for the simulations LESshear and LESmode. See caption of Figure 1 for details.

in the range of the higher rates provided in the literature.[6] Therefore, the discrepancies in their respective core lengths reported in Table 3 can mainly be attributed to the shifted locations of the spreading starting points. For the LESmode simulation, the shear layer appears to develop even later and more slowly. Two regions of spreading are visible: the vorticity thickness grows rapidly up to $x \simeq 8r_0$, then the rate of growth progressively decreases to reach $d\delta_\omega/dx \simeq 0.18$ for $10r_0 \leq x \leq 12r_0$. This behaviour and this rate are in good agreement with measurements of Husain & Hussain[8] for transitional axisymmetric shear layers.

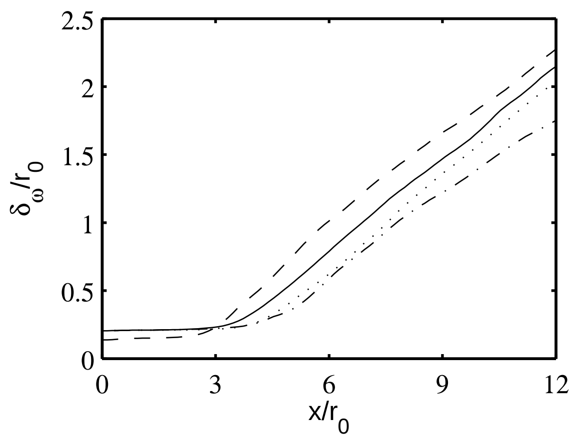

Figure 3: Axial evolution of vorticity thickness δ_ω. See Table 2 for the line types.

The u'-velocity spectra for $x = 3r_0$ and $r = r_0$ are presented in Figure 4 to investigate the preliminary stage of the shear layer development. They are marked by the instability waves growing in the inflow velocity profiles. The peak for LESshear is found for a Strouhal number $St \simeq 0.9$, those for LESac and LESampl for $St \simeq 0.6$. These values compare with the Strouhal numbers $St = 1.13$ and $St = 0.68$ associated with the most unstable, axisymmetric modes of the inflow shear layers predicted by the linear instability theory.[22] The discrepancies can be due to non-linear effects and to the differences between the velocity profiles at the inflow and at $x = 3r_0$. The peak amplitude is higher with the thinner initial shear layer which illustrates that the instability amplification is stronger as δ_θ decreases.[22] Using a smaller forcing magnitude in LESampl, the peak amplitude is only reduced with respect to LESac without affecting its frequency, suggesting that the same development occur. For LESmode, a less pronounced peak is observed for a lower Strouhal number $St \simeq 0.45$. This indicates

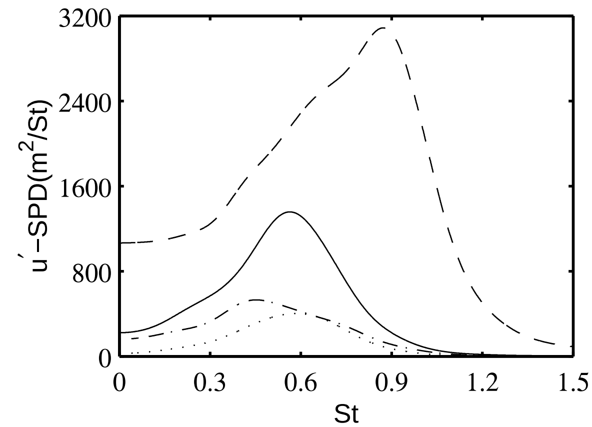

Figure 4: Spectral power densities of the u'-velocity as a function of Strouhal number $St = fD/u_j$, for $x = 3r_0$ and $r = r_0$, in linear scales. See Table 2 for the line types.

that the initial shear layer development may not be governed by the same instability modes.

The streamwise profiles for $r = r_0$ of the rms fluctuating axial and radial velocities are presented in Figures 5. The axial locations and the magnitudes of their peaks are investigated. For each of the three simulations LESshear, LESac and LESampl, the u'_{rms} and the v'_{rms} peaks occur at similar streamwise distances, respectively at $x \simeq 4.5r_0$, $x \simeq 6r_0$ and $x \simeq 7r_0$ according to the shifts in shear layer developments previously observed. For the LESmode simulation however, the two peaks do not coincide: u'_{rms} reaches its maximum value at $x \simeq 6r_0$ but v'_{rms} further downstream at $x \simeq 7r_0$.

The magnitudes of the peaks are given in Table 4. Similar peak values are found for the axial velocity, in fairly good agreement with measurements of Hussain & Zedan[7] reporting $(u'_{rms})_p/u_j \simeq 0.19$ in transitional axisymmetric shear layers. The peak values obtained for the radial velocity are more scattered, and all higher than the $(v'_{rms})_p/u_j \simeq 0.13$ measured by Hussain & Husain.[9] The ratios between the v'_{rms} and u'_{rms} peak magnitudes are also provided in Table 4. A ratio of about 0.92 is noted for the simulations LESac, LESampl and LESshear, whereas a smaller ratio is found for LESmode.

These results support that the turbulent shear layers have an identical structure for the three simulations using the same modal forcing. The magnitudes of velocity fluctuations are only slightly enhanced when the initial shear layer thickness is smaller or when the forcing amplitude is decreased. For the LESmode simulation, the turbulent shear layer

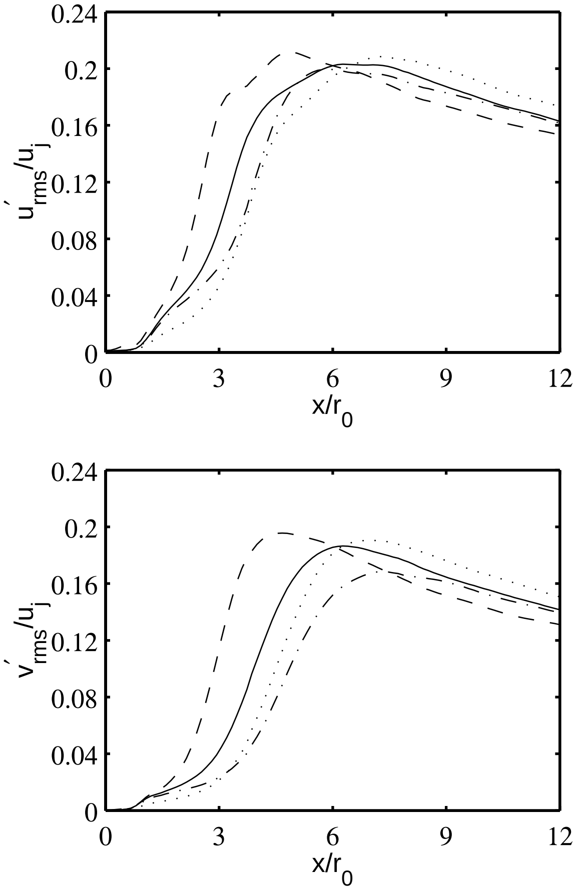

Figure 5: Axial profiles for $r = r_0$ of the rms-values of the fluctuating velocities u' and v'. See Table 2 for the line types.

displays quite different properties, with a spectacular reduction of the magnitude of the radial fluctuating velocity.

3.2 Jet developement

The influence of the inflow conditions on the jet development just after the potential core is now investigated. The streamwise evolutions of the mean centeline velocity u_c and of the jet-half width $\delta_{0.5}$ are presented in Figure 6 for the different simulations. The core lengths x_c arbitrarily defined by $u_c(x_c) = 0.95u_j$ are about $10r_0$ for LESac, LESampl and LESshear but $12r_0$ for LESmode, see Table 3 in section 2.3. They compare with those observed for untripped jets at similar Reynolds numbers by Raman *et al.*[10] and Arakeri *et al.*,[14] $x_c \simeq 10r_0$ and $x_c \simeq 14r_0$ respectively. They are all smaller than those found for higher Reynolds number, turbulent jets[23,24] yielding about $x_c \simeq 14r_0$. This result is in agreement with experiments of Raman *et al.*[10] showing that the potential core is shorter in an initially transitional jet than in an initially turbulent jet.

	$\frac{(u'_{rms})_p}{u_j}$	$\frac{(v'_{rms})_p}{u_j}$	$\frac{(v'_{rms})_p}{(u'_{rms})_p}$
LESac	0.203	0.186	0.92
LESampl	0.209	0.190	0.91
LESshear	0.212	0.196	0.92
LESmode	0.200	0.168	0.84

Table 4: Rms peak values of the fluctuating velocity profiles for $r = r_0$. The subscript p is used for *peak*.

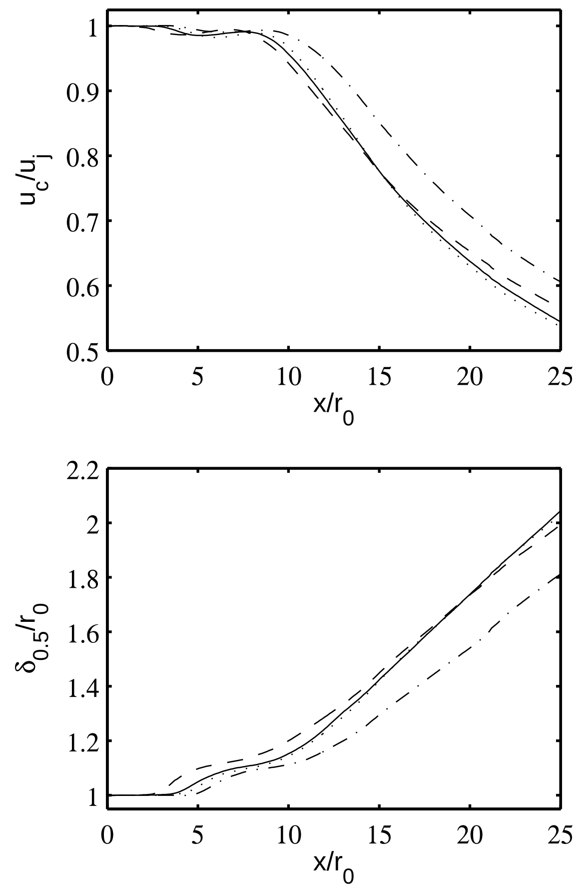

Figure 6: Axial profiles of the mean centerline velocity u_c/u_j and of the jet half-width $\delta_{0.5}/r_0$. See Table 2 for the line types.

The effects of the shear layer thickness and of the forcing amplitude on the centerline velocity decay and on the jet spreading are similar to the DNS results documented by Stanley & Sarkar[15] for a low Reynolds number plane jet. The jets for LESac and for LESampl using a smaller forcing amplitude develop at nearly the same rate. The decrease in the shear layer thickness for LESshear has a more significant impact on the jet development which clearly occurs at a lower rate than in LESac. For LESmode using the higher-mode excitation, the jet develops still more slowly. Considering experimental observations[10] that the spreading rate is higher in an initially transitional jet than in an initially turbulent jet, this may suggest that the jet excited with higher modes behave more as a turbulent jet than the other three. Note that no decay or spreading rate is provided here since these rates are significant only in the self-similarity region which is reached further downstream.[1,25]

The rms values of the axial and radial fluctuating velocities on the jet axis are plotted in Figure 7. For each of the four simulations, the peaks for u'_{rms} and for v'_{rms} are found at the same streamwise distance, around five radii downstream from the end of the potential core as observed experimentally in Arakeri *et al.*[14] for instance. The peak values are given in Table 5. They agree well with the experimental data, both for the axial and the radial velocities. For u'_{rms}/u_j, maxima of 0.13 and 0.12 were measured for similar Reynolds number, untripped jets[10,14] and maxima of 0.14 and 0.13 for $\mathrm{Re}_D = 10^6$ turbulent jets.[23,24] For v'_{rms}/u_j, peak values of 0.11 and 0.1 were reported in the latter cases.

The effects of the inflow conditions on the centerline turbulence peak values are well visible. The use in LESampl of a forcing amplitude smaller than in LESac enhances the turbulence peaks while this of a thinner initial shear layer in LESshear leads to a reduction, in accordance with the trends evidenced in the DNS of Stanley & Sarkar.[15] The forcing using higher modes in LESmode decreases the peak values both for u'_{rms} and for v'_{rms}. The ratios between the v'_{rms} and the u'_{rms} maxima are provided in Table 5. They are found to be 0.88 in LESmode and about 0.92 in the other simulations, which shows that the turbulence structure just after the potential core differs according to the modes involved in the inflow disturbances. The influence of the forcing modal properties on turbulence anisotropy appears however to be felt less strongly than earlier in the shear layer zones.

	$\frac{(u'_{rms})_p}{u_j}$	$\frac{(v'_{rms})_p}{u_j}$	$\frac{(v'_{rms})_p}{(u'_{rms})_p}$
LESac	0.131	0.118	0.90
LESampl	0.137	0.124	0.91
LESshear	0.122	0.113	0.91
LESmode	0.120	0.106	0.88

Table 5: Rms peak values of the centerline fluctuating velocity profiles. The subscript p is used for *peak*.

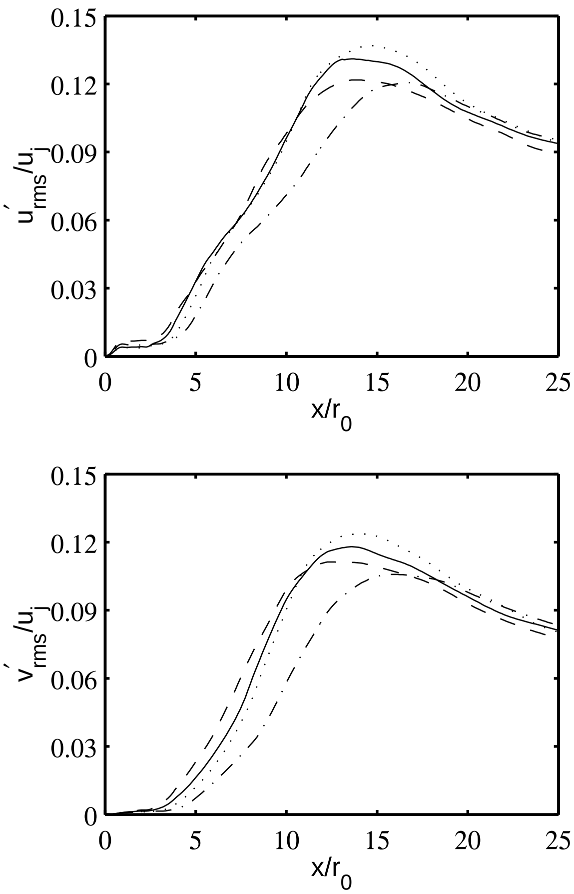

Figure 7: Centerline profiles of the rms-value of the fluctuating velocities u' and v'. See Table 2 for the line types.

4. Acoustic fields

4.1 Overall sound pressure levels

The profiles for $r = 15r_0$ of the sound pressure levels given directly from the LES are presented in Figure 8. The effects of the inflow conditions on the amplitude of the radiated noise are clearly shown. The decrease of the forcing magnitude in LESampl results in an amplification of the sound field by about 1 dB with respect to LESac. This amplification appears almost uniform for $0 \leq x \leq 30r_0$. The modification of the sound field when using a thinner shear-layer momentum thickness is different. The sound levels in LESshear are increased with respect to LESac for $x \leq 24r_0$, but they are reduced further downstream for $x \geq 24r_0$. This change according to the direction of sound emission will lead us to investigate in next subsections the properties of the sound field in the downstream and in the sideline directions where two distinct noise components are likely to be respectively dominant.[26] A significant noise reduction by about 2 dB is obtained in the LESmode simulation using a higher mode excitation. This result corresponds well to the behaviour found by Bodony & Lele[16] who reported that forcing using only the first three azimuthal modes is not sufficient and yields overestimated noise levels. At this point, it should be emphasized that the sound levels are shown to appreciably depend on the different inflow parameters. Since they appear also dependent on the subgrid modellings,[19] a great care is to be taken when using the SPL for demonstrating the validity of a jet noise prediction by LES.

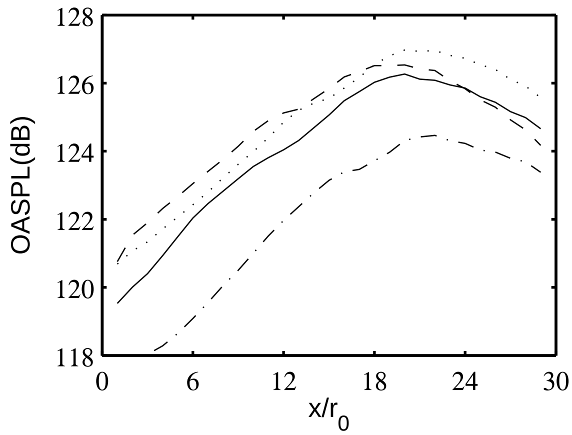

Figure 8: Overall sound pressure levels for $r = 15r_0$. See Table 2 for the line types.

4.2 Downstream noise properties

Spectra and azimuthal correlation functions of the acoustic fields are calculated for $x = 29r_0$ and $r = 12r_0$ as in an earlier paper.[1] They are presented in Figure 9. The shapes of the spectra are quite similar, with peaks observed for Strouhal numbers $St \simeq 0.3$ in agreement with experimental data.[24,27] Obtaining very close peak frequencies in the four simulations suggests that the mechanism at the origin of the downstream noise is the same whatever the inflow conditions may be. This is also supported by the cross correlation functions of the fluctuating pressure $R_{pp}(\phi)$ which display no significant differences according to the initial conditions. These correlation functions are typical[1] of measurements[28] for angles $\theta \simeq 30^o$ from the jet axis. One can also note from these functions that the more correlated the sound field, the higher the peak amplitude appears.

The sound levels calculated from the spectra at $x = 29r_0$ and $r = 12r_0$ are given in Table 6. They are higher for LESampl, and smaller for LESshear and LESmode, as already observed from the sound spectra. For a simple comparison with experiments, the sound levels are extrapolated at a distance $d = 60r_0$ from a source region assumed to be at $x = 10r_0$ on the jet axis at the end of the potential core.[2] The radiation angle thus defined from the jet axis is $\theta \simeq 30^o$. The levels are calculated using the $1/d$ decay law of sound waves and they are given in Table 6. They agree with the measurements for Mach 0.9, high Reynolds number jets at $\theta \simeq 30^o$ (Jordan *et al.*[24]: 115.5 dB, Mollo-Christensen *et al.*[27]: 116.3 dB, Tanna[29]: 114.6 dB) even if the 118 dB level predicted by the LESampl simulation seems slightly overestimated.

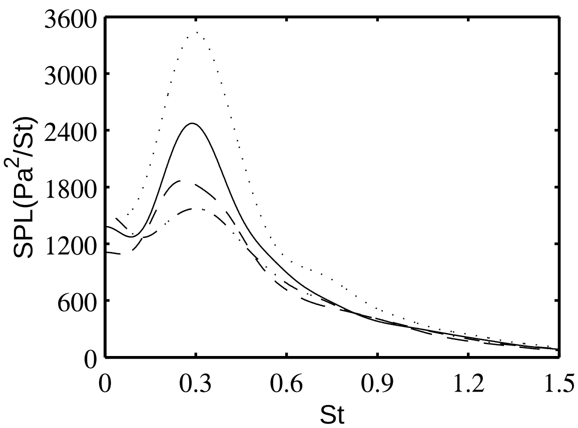

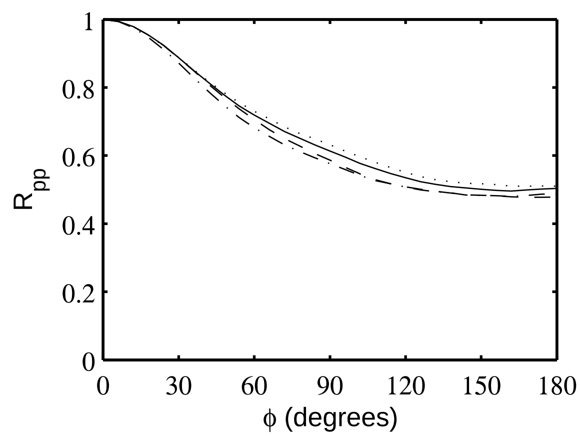

Figure 9: Top: sound pressure spectra in linear scales as a function of Strouhal number $St = fD/u_j$, bottom: azimuthal cross correlations of the fluctuating pressure, for $x = 29r_0$ and $r = 12r_0$. See Table 2 for the line types.

An attempt is conducted to connect the noise to the flow disturbance magnitude. This idea was developed particularly by Zaman[30] who showed that the noise sources in a M = 0.5, $\mathrm{Re}_D = 3 \times 10^5$ jet could be represented by the turbulence maxima loca-

	$\left\{ \begin{array}{l} x = 29r_0 \\ r = 12r_0 \end{array} \right.$	$\left\{ \begin{array}{l} d = 60r_0 \\ \theta \simeq 30^o \end{array} \right.$
LESac	125.2	116.7
LESampl	126.5	118
LESshear	124.5	116
LESmode	124.5	116

Table 6: Sound pressure levels in dB. Left: for $x = 29r_0$ and $r = 12r_0$, right: for $\theta \simeq 30^o$ at a distance $d = 60r_0$ from an origin taken as $x = 10r_0$ and $r = 0$, using the $1/d$ decay law.

tions. Arakeri *et al.*[14] using microjets for a M = 0.9 jet also observed that the reduction of the sound levels comes with the decrease of the turbulence intensities. Since the sources responsible for the downstream noise are expected to be located just after the end of the potential core,[2] our attention is turned to the peaks of centerline turbulence intensities which occur about two diameters after the jet core. The variations of the centerline turbulence maxima, earlier shown in Figure 7 and reported in Table 5, are found to exactly follow those of the peak values for $St \simeq 0.3$ in the sound spectra. This observation supports that the downstream noise component is associated with the turbulence intruding into the jet after the end of the potential core.[2] The downstream sound levels then appear only a function of the centerline turbulence intensity maxima.

4.3 Sideline noise properties

The properties of the sound fields in the sideline direction are now investigated. For high Reynolds number jets, they differ significantly from those in the downstream direction, in terms of spectral contents[31] and azimuthal correlations[28] . This important behaviour was shown to be obtained in the present LES.[1]

Sound spectra and cross correlation functions are calculated for $x = 11r_0$ and $r = 15r_0$, and presented in Figure 10. The four spectra display similar broadband shapes with peaks for Strouhal numbers $St \simeq 0.6 - 0.7$. The azimuthal correlation functions shown for $0 \leq \phi \leq 60^o$ are also very close, which supports that the same sound generation mechanisms take place in the four simulations. The decrease of the shear-layer thickness in LESshear enhances the sideline high-frequency noise, as expected since this noise component is mainly generated in the shear layers just after the nozzle exit.[30] The use of a smaller forcing amplitude in LESampl increases also slightly the acoustic levels. However the most striking change with respect to LESac is obtained from the LESmode simulation with a significant noise reduction.

The levels calculated from the previous spectra are given in Table 7. They are roughly extrapolated in the far-field, using the $1/d$ decay law of acoustic waves from an arbitrary source region. After a careful examination of the snapshots of pressure fields in Figures 1 and 2, the origin is chosen to be at $x = 7r_0$ on the jet axis. It defines an angle of sound emission from the jet axis of $\theta \simeq 75^o$. The sound levels extrapolated at a distance $d = 60r_0$ are provided in Table 7. They are found to be about 4 dB higher than the corresponding measurements at $\theta \simeq 75^o$ (Jordan *et al.*[24]: 106 dB, Mollo-Christensen *et al.*[27]: 108.2 dB, Tanna[29]: 108.3 dB), the 110 dB level provided by the LESmode simulation being the closer.

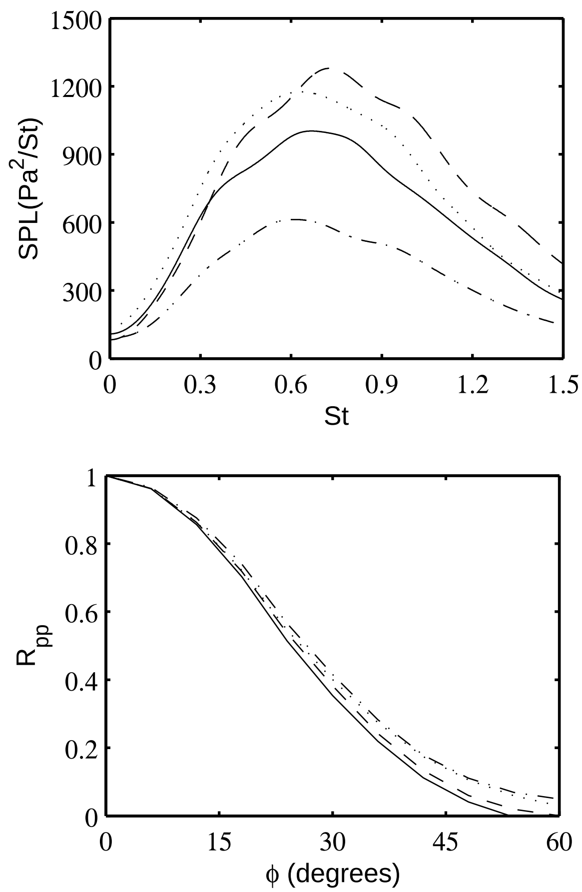

Figure 10: Top: sound pressure spectra in linear scales as a function of Strouhal number $St = fD/u_j$, bottom: azimuthal cross correlations of the fluctuating pressure, for $x = 11r_0$ and $r = 15r_0$. See Table 2 for the line types.

Since the shear layer turbulence is expected to contribute appreciably to the sideline noise, it seems natural to relate the present overestimated sound levels to the excessive magnitudes of the radial velocity fluctuations in the shear layer. It is found that the sound levels of Table 7 vary accurately as the maxima of v'_{rms} presented in Figure 5 and given in Table 4. The sideline noise is shown to be linked with the intensity of the radial velocity disturbances in the shear layer. For predicting sideline noise levels in numerical simulations in agreement with measurements, it appears then necessary to still define an inflow forcing reducing this quantity. The results from the LESmode simulation suggest however that the first jet modes should not be involved when synthesizing the the initial perturbations.

	$\begin{cases} x = 11r_0 \\ r = 15r_0 \end{cases}$	$\begin{cases} d = 60r_0 \\ \theta \simeq 75^o \end{cases}$
LESac	124.1	112.3
LESampl	124.7	113
LESshear	125.2	113.4
LESmode	121.8	110

Table 7: Sound pressure levels in dB. Left: for $x = 11r_0$ and $r = 15r_0$, right: for $\theta \simeq 75^o$ at a distance $d = 60r_0$ from an origin taken as $x = 7r_0$ and $r = 0$, using the $1/d$ decay law.

5. Conclusion

This paper describes effects of the inflow conditions for a high subsonic, $\mathrm{Re}_D = 4 \times 10^5$ circular jet simulated by Large Eddy Simulation. Both the flow development and the emitted sound are shown to depend appreciably on the initial parameters chosen to model the inflow of this transitional jet.

The reduction of the amplitude of the initial disturbances is found to alter the flow and sound properties only weakly and in the following way: the jet development occurs slightly downstream with higher turbulence intensities, and consequently an increased radiated noise. The use of a thinner shear-layer momentum thickness leads to more significant and complex modifications. The transition is more rapid and turbulence intensities are increased in the shear layer, but the jet developement is slower and the intensities are decreased after the potential core. As a result, noise is enhanced in the sideline direction but reduced in the downstream direction. The most important changes in the flow features are obtained with the removing of the first four jet azimuthal modes in the building of the inflow disturbances: the jet develops much later and slowly, turbulence intensities and noise levels are notably reduced. This work demonstrates the importance of the modelling of the inflow conditions for high Reynolds number jets. In particular, initial conditions are still to be tested to reduce the sideline pressure levels which are overestimated with respect to experimental data. This discrepancy has moreover been connected to the high intensity of the radial fluctuating velocity in the shear layer.

Strong links between the turbulence and the sound radiation are indeed suggested by the present simulations. The levels of the downstream noise dominated by a $St \simeq 0.3$ peak can be related to the maxima of centerline intensities just after the potential core, which supports that the associated generation mechanism is effectively located in this zone. The amplitudes of the sideline noise are also found to be connected to the peak values of the radial velocity fluctuations in the shear layer. The broadband noise generated in the sideline direction for jets at high Reynolds numbers is thus shown to be direcly associated to the development of the shear-layer turbulence.

Acknowledgments

A part of this work was supported by the EU Research programme JEAN (Jet Exhaust Aerodynamics and Noise) (Contract No. G4RD-CT-2000-00313). Computing time is supplied by Institut du Développement et des Ressources en Informatique Scientifique (IDRIS - CNRS).

References

[1] Bogey, C. & Bailly, C., 2002, Direct computation of the sound radiated by a high Reynolds number, subsonic round jet, *CEAS Workshop From CFD to CAA*, 7-8 Nov., Athens, Greece.

[2] Bogey, C., Bailly, C. & Juvé, D., 2003, Noise investigation of a high subsonic, moderate Reynolds number jet using a compressible LES, *Theoret. Comput. Fluid Dynamics*, **16**(4), 273-297.

[3] Crighton, D.G., 1981, Acoustics as a branch of fluid mechanics, *J. Fluid Mech.*, **106**, 261-298.

[4] Zaman, K.B.M.Q., 1985, Far-field noise of a subsonic jet under controlled excitation, *J. Fluid Mech.*, **152**, 83-111.

[5] Hill, W.G., Jr., Jenkins, R.C. & Gilbert, B.L., 1976, Effects of the initial boundary-layer state on turbulent mixing, *AIAA Journal*, **14**(11), 1513-1514.

[6] Gutmark, E. & Ho, C.-M., 1983, Preferred modes and the spreading rates of jet, *Phys. Fluids*, **26**(10), 2932-2938.

[7]HUSSAIN, A.K.M.F. & ZEDAN, M.F., 1978, Effects of the initial condition on the axisymmetric free shear layer: Effects of the initial momentum thickness, *Phys. Fluids*, **21**(7), 1100-1112.

[8]HUSAIN, Z.D. & HUSSAIN, A.K.M.F., 1979, Axisymmetric mixing layer: influence of the initial and boundary conditions, *AIAA Journal*, **17**(1), 48-55.

[9]HUSSAIN, A.K.M.F. & HUSAIN, Z.D. , 1980, Turbulence structure in the axisymmetric free mixing layer, *AIAA Journal*, **18**(12), 1462-1469.

[10]RAMAN, G., RICE, E.J. & RESHOTKO, E., 1994, Mode spectra of natural disturbances in a circular jet and the effect of acoustic forcing, *Experiments in Fluids*, **17**, 415-426.

[11]XU, G. & ANTONIA, R.A., 2002, Effects of different initial conditions on a turbulent free jet, *Experiments in Fluids*, **33**, 677-683.

[12]BRIDGES, J.E. & HUSSAIN, A.K.M.F., 1987, Roles of initial conditions and vortex pairing in jet noise, *J. Sound Vib.*, **117**(2), 289-311.

[13]SIMONICH, J.C., NARAYANAN, S., BARBER, T.J. & NISHIMURA, M., 2001, Aeroacoustic characterization, noise reduction, and dimensional scaling effects of high subsonic jets, *AIAA Journal*, **39**(11), 2062-2069.

[14]ARAKERI, V.H., KROTHAPALLI, A., SIDDAVARAM, V., ALKISLAR, M.B. & LOURENCO, L., 2002, Turbulence suppression in the noise producing region of a Mach=0.9 jet, AIAA Paper 2002-2523.

[15]STANLEY, S.A. & SARKAR, S., 2000, Influence of nozzle conditions and discrete forcing on turbulent planar jets, *AIAA Journal*, **38**(9), 1615-1623.

[16]BODONY, D.J. & LELE, S.K., 2002, Influence of inlet conditions on the radiated noise of high speed turbulent jets, *Workshop LES for Acoustics*, 7-8 Oct., DLR Göttingen, Germany. See also CONSTANTINESCU & LELE, AIAA Paper 2001-0376.

[17]CHYCZEWSKI, T.S., LONG, L.N. & MORRIS, P.J., 1998, Numerical study of nozzle exit conditions effects on jet development, *AIAA Journal*, **36**(6), 986-993.

[18]BOERSMA, B.J., BRETHOUWER, G. & NIEUWSTADT, F.T.M., 1998, A numerical investigation on the effect of the inflow conditions on a self-similar region of a round jet, *Phys. Fluids*, **10**(4), 899-909.

[19]BOGEY, C. & BAILLY, C., 2003, LES of a high Reynolds, high subsonic jet : effects of the subgrid modellings on flow and noise, *16th AIAA CFD Conference*, 23-26 June, Orlando, USA, AIAA Paper 2003-3557.

[20]BOGEY, C. & BAILLY, C., 2002, A family of low dispersive and low dissipative explicit schemes for computing the aerodynamic noise, AIAA Paper 2002-2509.

[21]BOGEY, C. & BAILLY, C., 2002, Three-dimensional non reflective boundary conditions for acoustic simulations: far-field formulation and validation test cases, *Acta Acustica*, **88**(4), 463-471.

[22]MICHALKE, A., 1984, Survey on jet instability theory, *Prog. Aerospace Sci.*, **21**, 159-199.

[23]LAU, J.C., MORRIS, P.J. & FISHER, M.J., 1979, Measurements in subsonic and supersonic free jets using a laser velocimeter, *J. Fluid Mech.*, **93**(1), 1-27.

[24]JORDAN, P., GERVAIS, Y., VALIÈRE, J.-C. & FOULON, H., 2002, Final results from single point measurements, *Project deliverable D3.4, JEAN - EU 5th Framework Programme, G4RD-CT2000-00313.*

[25]WYGNANSKI, I. & FIEDLER, H., 1969, Some measurements in the self-preserving jet, *J. Fluid Mech.*, **38**(3), 577-612.

[26]TAM, C.K.W., GOLEBIOWSKI, M. & SEINER, J.M., 1996, On the two components of turbulent mixing noise from supersonic jets, AIAA Paper 96-1716.

[27]MOLLO-CHRISTENSEN, E., KOLPIN, M.A. & MARTUCELLI, J.R., 1964, Experiments on jet flows and jet noise far-field spectra and directivity patterns, *J. Fluid Mech.*, **18**, 285-301.

[28]MAESTRELLO, L., 1976, Two points correlations of sound pressure in the far field of a jet: Experiment, NASA-TMX-72835.

[29]TANNA, H.K., 1977, An experimental study of jet noise. Part I: Turbulent mixing noise. *J. Sound Vib.*, **50**(3), 405-428.

[30]ZAMAN, K.B.M.Q., 1986, Flow field and near and far sound field of a subsonic jet, *J. Sound Vib.*, **106**(1), 1-16.

[31]LUSH, P.A., 1971, Measurements of subsonic jet noise and comparison with theory, *J. Fluid Mech.*, **46**(3), 477-500.